4. A Prediction Method for Ship Viscous Resistance by Boundary Layer Theory

Yoji HIMENO,* *Member* and Tatsushi ISHII,** *Member*

(*From J.S.N.A. Japan, Vol. 154, December 1983*)

Summary

A simple integral-type boundary-layer calculation method is applied to the prediction of ship viscous resistance. A calculation method for the vortex resistance due to the stern bilge vortex is evaluated from the energy-loss concept using the crossflow quantities in the stern boundary layer. The ship viscous resistance thus consists both of the streamwise momentum loss and of the cross flow energy loss. A regression analysis of the resistance shows a fairly good agreement between the theory and experiments.

The local development of the viscous resistance components near stern is also discussed in terms of the boundary layer quantities. The potential-flow quantities like pressure gradient and streamline convergence are related to the boundary layer development and then the viscous resistance. The present method can be applied to ship stern form improvement for reducing viscous resistance.

1. Introduction

Among the calculation methods of ship boundary layer, kinds of the second order theory which take into account the effect of pressure field on the stern boundary layer development, like Soejima,[1] Nagamatsu,[2] and Muraoka,[3] seem at present to be most prospective. However, more effort would be necessary for the prediction of the velocity field near propeller disk even by these methods.

On the other hand, it is also important to use existing simple integral methods, like Hatano,[4] Himeno,[5] Tanaka,[6] and Okuno's[7] methods for the improvement of ship stern hull form, for the prediction of stern flow in the region between SS3 to SS1, and for the analysis of ship hull roughness, etc. The present paper stands on the latter point of view, and proposes a new method of predicting ship viscous resistance using the simple boundary layer theory.

Many attempts have so far been done to predict the ship viscous resistance by the use of Squire and Young's method,[8] like Hatano,[9] Uberoi,[10] Nagamatsu,[11] Granville,[12] Hess[13] and Hoffman.[14] These methods, however, do not take into account the bilge vortex effect. Sasajima *et al.*,[15] Tatinclaux,[16] and Tanaka[17] made an estimation of the bilge-vortex resistnace component from the measured crossflow values and pointed it can not be negligible, though small compared to the total viscous resistance. Bessho[18),19),20] made a theoretical analysis on the vortex resistance which is estimated as an energy loss in a ship hull section due to the potential crossflow along girth line.

In the present analysis, the longitudinal vortex is assumed to be the crossflow in the ship boundary layer and the viscous resistance is assumed to be the sum of the streamwise momentum loss derived from Squire and

* University of Osaka Prefecture, College of Engineering

** Graduate student, University of Osaka Prefecture

Young's method and the crossflow energy loss expressed as an integration form using boundary layer quantities. In chapter 2 and 3 the discussions of the viscous resistance are stated, the relation of the boundary layer characteristics and the stern hull form is discussed in chapter 4, and in chapter 5 an application of the present analysis to the ship form series SR-183[21] and SR-61[22] are shown.

2. Preliminary Consideration of Vortex Resistance

To clarify the meaning of the term "vortex resistance," the analysis of momentum balance in a wake with a swirl motion is carried out.

Let an axisymmetric coordinate system (x, r, θ) be defined as in Fig. 1 in a far downstream of a body, in which U represents the uniform stream, u the wake velocity loss, v the swirling velocity due to a longitudinal vortex. Put the origin of x at the starting point of the wake. The present analysis starts with the same sense in the Rosenhead's text book.[23] The equation for the viscous wake is expressed in the form,

$$(U-u)\frac{\partial u}{\partial x}+w\frac{\partial u}{\partial r}=\frac{1}{\rho}\frac{\partial p}{\partial x}+\nu\left(\frac{\partial^2 u}{\partial r^2}+\frac{1}{r}\frac{\partial u}{\partial r}\right) \tag{2.1}$$

$$\frac{v^2}{r}=\frac{1}{\rho}\frac{\partial p}{\partial r} \tag{2.2}$$

$$(U-u)\frac{\partial v}{\partial x}+w\frac{\partial v}{\partial r}+\frac{vw}{r}=\nu\left(\frac{\partial^2 v}{\partial r^2}+\frac{1}{r}\frac{\partial v}{\partial r}-\frac{v}{r^2}\right) \tag{2.3}$$

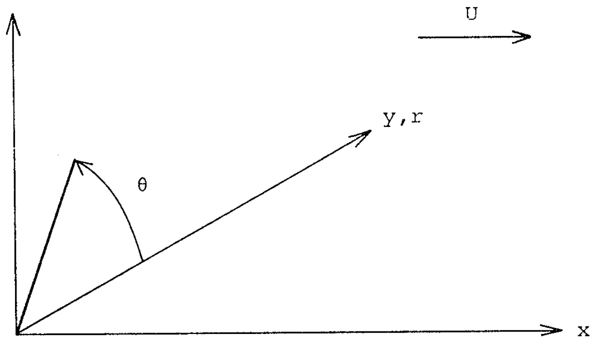

Fig. 1 Coordinates for infinite wake

$$-\frac{\partial}{\partial x}(ru)+\frac{\partial}{\partial r}(rw)=0 \tag{2.4}$$

with the following boundary condition.

$$\left.\begin{array}{l}\text{for}\quad r=0,\ v=w=0\\ \text{for}\quad r\to\infty,\ u\to 0,\ v\to 0,\ p\to p_0\end{array}\right\} \tag{2.5}$$

Eq. (2.2) shows a balance between the centrifugal force and the pressure. It can be derived from integrating the above equations that there are three constants in this system, i.e., the reistance R, the flux Q, and the angular momentum M as follows.

$$R=2\pi\int_0^\infty r\{(p_0-p)+\rho u(U-u)\}dr=\text{const.} \tag{2.6}$$

$$Q=2\pi\int_0^\infty rudr=\text{const.} \tag{2.7}$$

$$M=2\pi\rho\int_0^\infty r^2v(U-u)dr=\text{const.} \tag{2.8}$$

However, the circulation Γ due to the swirl is not conserved in this wake flow model. These constants should be prescribed by the body located in front of the wake, so that they can be used as the integration constants when the equations are solved.

We assume the velocities u, v, and w are small compared to U and define a variable η as the form.

$$\eta=r\sqrt{\frac{U}{4\nu x}} \tag{2.9}$$

And assuming the damping rate of the velocities as

$$u\propto x^{-m}f(\eta)\ ,\quad v\propto x^{-n}g(\eta) \tag{2.10}$$

we can determine the factors from eqs. (2.2), (2.4), (2.6) and (2.8) as follows.

$$u\propto x^{-1}f(\eta),\quad v\propto x^{-3/2}g(\eta),\quad w\propto x^{-3/2},\quad p\propto x^{-3} \tag{2.11}$$

The variables v, w, and p thus damp out faster than u. If we expand the solutions as

$$\left.\begin{array}{ll}u=u_1+u_2+\cdots, & v=v_1+v_2+\cdots\\ w=w_1+w_2+\cdots, & p=p_1+p_2+\cdots\end{array}\right\} \tag{2.12}$$

the orders of damping should be the following.

$$\left.\begin{array}{l}O(u_1)=O(x^{-1}),\quad O(v_1)=O(w_1)=O(x^{-3/2})\\ O(p_1)=O(x^{-3})\end{array}\right\} \tag{2.13}$$

Therefore, only the term u_1 is of the first order and its solution is well known as an axisymmetric wake. From eq. (2.1) we obtain

$$U\frac{\partial u_1}{\partial x}=\frac{\nu}{r}\frac{\partial}{\partial r}\left(r\frac{\partial u_1}{\partial r}\right) \tag{2.14}$$

and putting eq. (2.11) the equation for f is written as

$$(\eta f')'+2\eta^2 f'+4\eta f=0 \tag{2.15}$$

with the boundary conditions that $f=0$ at center and infinity. The solution is expressed as

$$u_1=\frac{R_1}{4\pi\rho\nu x}e^{-\eta^2} \tag{2.16}$$

where the constant R_1 is given as

$$R_1=2\pi\rho U\int_0^\infty ru_1dr=\rho UQ_1 \tag{2.17}$$

This first order solution is well known and does not include the effects of the swirl nor the pressure.

We can proceed on the second order solutions. First for u_2 we obtain the following form from eq. (2.1).

$$U\frac{\partial u_2}{\partial x}-\frac{\nu}{r}\frac{\partial}{\partial r}\left(r\frac{\partial u_2}{\partial r}\right)$$
$$=u_1\frac{\partial u_1}{\partial x}-w_1\frac{\partial u_1}{\partial r}+\frac{1}{\rho}\frac{\partial p_1}{\partial x} \tag{2.18}$$

If we treat the righthand side of eq. (2.18) separately as the inertia effect and the pressure effect, we can first assume the solution for the inertia effect as

$$u_2=\frac{UA_2}{x^2}f_2(\eta) \tag{2.19}$$

and the equation for f_2 becomes the form.

$$(\eta f_2')'+2\eta^2 f_2'+8\eta f_2=\eta e^{-2\eta^2} \tag{2.20}$$

The solution is expressed as

$$u_2=\frac{A_1^2}{x^2}e^{-2\eta^2}\left(\eta^2+\frac{3}{4}\eta^4+\cdots\right) \tag{2.21}$$

Putting u_2 into eq. (2.18) excluding the pressure term and integrating we obtain

$$2\pi\rho\int_0^\infty rUu_2dr=2\pi\rho\int_0^\infty ru_1^2dr \tag{2.22}$$

When we compare the above equation to the expansion of eq. (2.6)

$$R=2\pi\rho\int_0^\infty rUu_1dr-2\pi\rho\int_0^\infty u_1^2rdr$$
$$+2\pi\rho\int_0^\infty rUu_2dr+\cdots+2\pi\int(p-p_1)rdr \tag{2.23}$$

we can see that the resistance due to u_2 compensates with the higher order term of u_1, and that the higher order inertia terms do not contribute for resistance.

We next consider the pressure effect in eq. (2.18). Beforehand, we have to obtain the solutions for p and v. Expanding eq. (2.3) we obtain

$$U\frac{\partial v_1}{\partial x}=\nu\left(\frac{\partial^2 v_1}{\partial r^2}+\frac{1}{r}\frac{\partial v_1}{\partial r}-\frac{v_1}{r^2}\right) \tag{2.24}$$

and assume

$$v_1=Bx^{-3/2}g(\eta) \tag{2.25}$$

then the equation for the similar profile for v_1 is

$$\eta^2 g''+(2\eta^3+\eta)g'+(6\eta^2-1)g=0 \tag{2.26}$$

The solution can easily be obtained as

$$v_1=\frac{M_1}{16\pi\rho U}\left(\frac{U}{\nu x}\right)^{3/2}\eta e^{-\eta^2} \tag{2.27}$$

in which the constant M_1 is the first order term of M in eq. (2.8). The pressure p_1 is derived from eq. (2.2).

$$p_1-p_0=-\frac{\rho U^2}{102\pi^2}\left(\frac{M_1}{\rho U^2}\right)^2\left(\frac{U}{\nu x}\right)^3 e^{-2\eta^2} \tag{2.28}$$

The profiles for v_1 and p_1 are quite analogous to Rankine model. For the pressure effect on u in eq. (2.18), the form of u_2 should be expressed as

$$u_2=\frac{UA_2}{x^3}f(\eta) \tag{2.29}$$

which means the pressure effect is of the third order. The solution can be obtained as the form.

$$u_2=-\frac{U}{256\pi^2}\left(\frac{M_1}{\rho U^2}\right)^2\left(\frac{U}{\nu x}\right)^2 e^{-2\eta^2}\left\{\frac{1}{4}\right.$$
$$\left.+\frac{1}{2}\eta^2+\frac{1}{64}\eta^4+\cdots\right\} \tag{2.30}$$

We thus realize the situation that the swirling flow v_1 which damps as $O(x^{-3/2})$ creates the pressure drop of $O(x^{-3})$ and leads to the velocity increment u_2 in eq. (2.30).

This relation is also confirmed in the momentum balance. The effect of vortex flow corresponds to the pressure term in eq. (2.23) which we can define as R_{VOR}.

$$R_{VOR}=2\pi\int(p_0-p_1)rdr=\frac{\rho U^2}{512\pi}\left(\frac{M_1}{\rho Uxv}\right)^2 \tag{2.31}$$

Further defining R_2 as the resistance component due to u_2 in eq. (2.30), i.e., the pressure effect, then from eq. (2.23) we obtain

$$R=2\pi\rho\int rUu_1dr+2\pi\rho\int rUu_2dr$$
$$+2\pi\int(p_0-p)rdr=R_1+R_2+R_{VOR} \tag{2.32}$$

in which the inertia effect has been omitted. If we integrate eq. (2.18) excluding the inertia terms of u_1, we also obtain

$$R_2=-R_{VOR} \tag{2.33}$$

which means the pressure resistance due to swirl R_{VOR} balances the corresponding momentum increment R_2. Then the immediate result is $R=R_1$ which seems there is no influence of vortex. However, the velocities u_1 and u_2 can not be separated in actual flow. Therefore the sum of R_1 and R_2, i.e.,

$$R_{MOM}=R_1+R_2 \tag{2.34}$$

is only the measurable quantity, and the expression

$$R=R_{MOM}+R_{VOR} \tag{2.35}$$

can be considered as a meaningful form. In this case an integration of eqs. (2.2) and (2.31)

$$R_{VOR}=\int_0^\infty\frac{\rho}{2}v_1^2\cdot 2\pi rdr \tag{2.36}$$

corresponds to the ordinary definition of the vortex resistance.

$$R_{VOR}=\int\frac{\rho}{2}(v_y^2+v_z^2)dA \tag{2.37}$$

The vortex resistance R_{VOR} damps as $O(x^{-2})$ in the wake and the momentum-loss resistance R_{MOM} increases correspondingly. In engineering sense, however, we can define R_{VOR} as its maximum. The present analysis on the simple wake model can reasonably be applied to the ship stern wake flow in which the swirling flow due to longitudinal vortex corresponds to the vortex resistance R_{VOR}.

3. Method for Predicting Viscous Resistance

The authors proposes here a method of calculating the two components R_{MOM} and R_{VOR} in the preceding section by using the solutions of the ordinary first order boundary layer theory. Take the streamline coordinates (s, n, ζ) as in Fig. 2, where n represents equipotential line and ζ the outward normal. We assume the boundary layer equations continue to hold in the wake region.

For the streamwise momentum-loss resistance R_{MOM}, we can adopt the ordinary Squire and Young's formula[8] as used in common.

$$R_{MOM}=\rho U^2\int\theta_\infty dn_\infty \tag{3.1}$$

The subscript "∞" represents the infinite downstream. Neglecting the streamline curva-

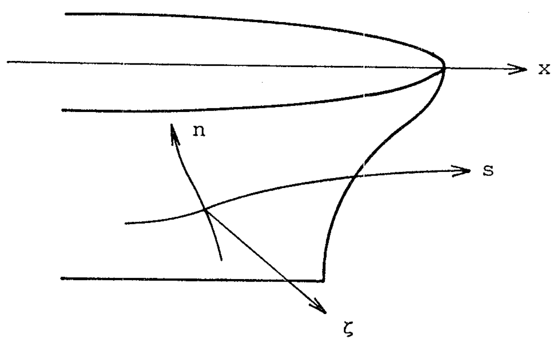

Fig. 2 Streamline coordinates

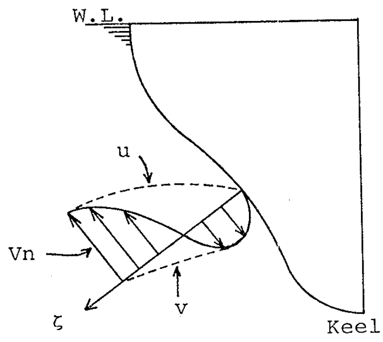

Fig. 3 Crossplane flow component

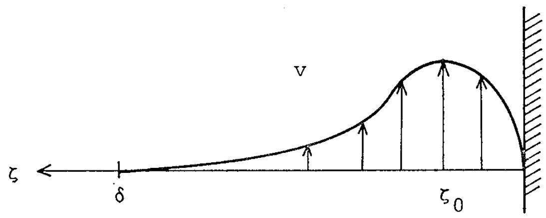

Fig. 4 Crossflow profile

ture K_2 in the wake region, we can convert the integral to the stern region.

$$R_{MOM}=\rho U^2\int_{\text{girth}}\theta\left(\frac{U_e}{U}\right)^{(H+5)/2}dn \quad (3.2)$$

The value can be taken as its maximum over stern sections and the variable n as the girth coordinate at the section considered.

For the longitudinal vortex, we assume it is an appearance of the vorticity in the boundary layer. From Fig. 2 we obtain

$$\omega_x=\omega_s\frac{\partial s}{\partial x}+\omega_n\frac{\partial n}{\partial x} \quad (3.3)$$

in which the vorticity component along the normal is neglected. Within the boundary layer approximation we can assume

$$\omega_s=-\frac{\partial v}{\partial\zeta}, \quad \omega_n=\frac{\partial u}{\partial\zeta} \quad (3.4)$$

which means that the components ω_s and ω_n are the contributions of the crossflow and the streamwise velocity loss respectively, as shown in Fig. 3. For the cross flow component, the integration of the vorticity from a point close to wall to the outer edge, as shown in Fig. 4, gives a circulation density γ_s per unit girth length.

$$\gamma_s=-\int_{\zeta_0}^{\delta}\omega_s ds=-v(\zeta_0) \quad (3.5)$$

Similarly, the circulation γ_{nx} which is a projection of the n-component to x-axis, can be obtained as follows.

$$\gamma_s=-\int_0^{\delta}\omega_n\cdot\frac{\partial n}{\partial x}d\zeta=-U_e\frac{\partial n}{\partial x}\fallingdotseq V_n \quad (3.6)$$

Therefore, assuming $\partial s/\partial x$ nearly equal to unity, we obtain the form.

$$\gamma_x=\gamma_s+\gamma_{nx} \quad (3.7)$$

This means that the circulation consists of the upward velocity at the edge (γ_{nx}) and the downward velocity near wall (γ_s), in which the former is negligible in the wake by boundary layer assumption and the latter goes downstream but it also damps out in the wake downstream.[24] Therefore the maximum of γ_s takes place on the ship hull region. In the boundary layer region, the circulation density γ_s can be calculated by assuming power law and Mager model for the velocity profile,

$$\gamma_s=-kU_e\tan\beta_w, \quad k=\frac{16}{(H+3)^2}\left(\frac{H-1}{H+3}\right)^{(H-1)/2} \quad (3.8)$$

where β_w stands for the wall crossflow angle.

For estimating the vortex resistance, we assume that the circulation γ_s due to the crossflow is located along the girth line in a cross section and that it flows downstream along x-axis with the velocity U. So the crossflow energy in the Trefftz plane created by the circulation γ_s can be considered as a measure of the vortex energy, which is expressed as the form,

$$R_{VOR}=\frac{\rho}{2\pi}\iint_{\text{keel}}^{\text{WL}}\gamma_s(Z)\gamma_s(Z')\cdot\ln\left|\frac{(Z-\bar{Z}')(Z+\bar{Z}')}{(Z-Z')(Z+Z')}\right|dl'dl \quad (3.9)$$

where Z and Z' represent girth coordinates in complex form.

The total viscous resistance can thus be considered to be the sum of the preceding two components. For practical use, however, we have to introduce empirical constants to the expression of the viscous resistance as follows,

$$R_V=C_1R_{MOM}+C_2R_{VOR} \quad (3.10)$$

where the constants can be determined by fitting the present formula to some series model test data.

4. Stern Hull Form and Boundary Layer

The discussions in the preceding section indicates that the boundary layer calculation at ship stern is meaningful because it gives a distribution of the viscous resistance components over the hull. For instance, the expression,

$$\theta_\infty=\theta\left(\frac{U_e}{U}\right)^{(H+5)/2} \tag{4.1}$$

is interpreted as a density distribution of the momentum loss resistance R_{MOM}. Since the wall crossflow angle is proportional to the circulation density γ_s, its distribution on the hull determines the vortex resistance as in eq. (3.9). If we can control these factors by changing the hull configuration, that will be quite helpful for the improvement of ship hull form.

On the other hand, even a potential flow calculation, without solving boundary layer equations, would also be helpful for estimating the boundary layer development. A simple integral-type boundary layer equations can be written in the form.

$$\frac{\partial}{\partial s}(U_e^2\theta)+U_eH\theta\frac{\partial U_e}{\partial s}+\frac{\partial}{\partial n}(U_e^2\theta_{12})+U_e\delta_2\frac{\partial U_e}{\partial n}$$
$$-K_2U_e^2(\theta_{12}+\theta_{21})-K_1U_e^2(\theta-\theta_{22})=\frac{1}{2}c_fU_e^2 \tag{4.2}$$

$$\frac{\partial}{\partial n}(U_e^2\theta_{22})+\frac{\partial}{\partial s}(U_e^2\theta_{21})-2K_1U_e^2\theta_{21}$$
$$-K_2U_e^2(\theta_{22}-\theta-H\theta)=\frac{1}{2}c_fU_e^2\tan\beta_w \tag{4.3}$$

The thicknesses θ_{12}, θ_{22}, and δ_2 are related to the crossflow angle, and c_f, K_1, and K_2 represent, respectively, local wall friction coefficient, streamline convergence rate and streamline curvature. The small crossflow assumption gives the following form.

$$\frac{d\theta}{ds}-\frac{1}{2}c_f=\theta\left\{K_1-\frac{(H+2)}{U_e}\frac{\partial U_e}{\partial s}\right\} \tag{4.4}$$

$$\frac{d}{ds}(U_e^2\theta_{21})-2K_1U_e^2\theta_{21}-\frac{1}{2}c_fU_e^2\tan\beta_w$$
$$=K_2U_e^2\theta(H+1) \tag{4.5}$$

Neglecting the term c_f in the stern region and replacing $H+2$ to a constant, say, 3.3, the following factor

$$P_2=K_1-\frac{3.3}{U_e}\frac{\partial U_e}{\partial s} \tag{4.6}$$

represents a logarithmic rate of the growth of the momentum thickness. We shall hereafter call P_2 modified pressure gradient factor, which can be obtained by potential flow calculation. As Tanaka *et al.*[6] pointed out, the wall crossflow angle β_w depends highly on the value of the streamline curvature K_2 as is seen in eq. (4.5), which is also obtainable from inviscid calculation.

$$K_2=\frac{1}{U_e}\frac{\partial U_e}{\partial n} \tag{4.7}$$

Consequently, the boundary layer development and the viscous resistance distribution on the hull can roughly be estimated from the quantities P_2 and K_2 by potential flow calculation, which are also useful for ship hull improvement, as well as the boundary layer solutions.

5. Calculation Results and Discussions

The present method is applied to two series ship forms. One is named SR183 which includes 6 wide-beam small-draft hull forms with a stern bulb, except for the mother model SR183A. The principal dimensions are shown

Table 1 Principal dimensions of SR-183 models

M.S.No.	SR183A	SR183B	SR183C	SR183D	SR183E	SR183F
Lpp (m)			2.0250			
B (m)			0.4500			
d (m)			0.1324			
C_B	0.6040	0.6041	0.6039	0.6043	0.6054	0.6040
C_P	0.6227	0.6228	0.6226	0.6230	0.6241	0.6227
C_W	0.7583	0.7581	0.7581	0.7590	0.7927	0.7601
lcb	1.781	1.780	1.771	1.783	1.858	1.776
W.S. (m^2)	1.0339	1.0340	1.0386	1.0392	1.0668	1.0406

Shaft center height 48.8 mm , Fn=0.26 , Rn=2.046×10^6

Table 2 Principal dimensions of SR-61 models

M.S.No.	L(m)	L/B	B/d	C_B	lcb(%)	$(1-C_{pa})\frac{Lpp}{2B}$	W.S.(m^2)
1591	6.0	6.0	2.76	0.78	-1.491	0.740	8.550
1592*	6.0	6.0	2.76	0.80	-1.491	0.670	8.705
1593	6.0	6.0	2.76	0.82	-1.491	0.613	8.843
1594	6.0	6.0	2.76	0.84	-1.491	0.560	8.967
1657	6.0	5.5	3.06	0.82	-1.491	0.571	9.213
1659	6.0	5.75	3.06	0.82	-1.491	0.592	8.824
1661	6.0	6.0	3.06	0.82	-1.491	0.613	8.455
1658	6.0	5.5	2.76	0.82	-1.491	0.571	9.643
1660	6.0	5.75	2.76	0.82	-1.491	0.592	9.227
1751	6.0	6.0	2.76	0.80	-2.260	0.726	8.706
1752	6.0	6.0	2.76	0.80	-3.023	0.775	8.708
1753	6.0	6.0	2.76	0.80	-3.807	0.828	8.719

*) Mother form , Fn = 0.1 , Rn = 4.091×10^6

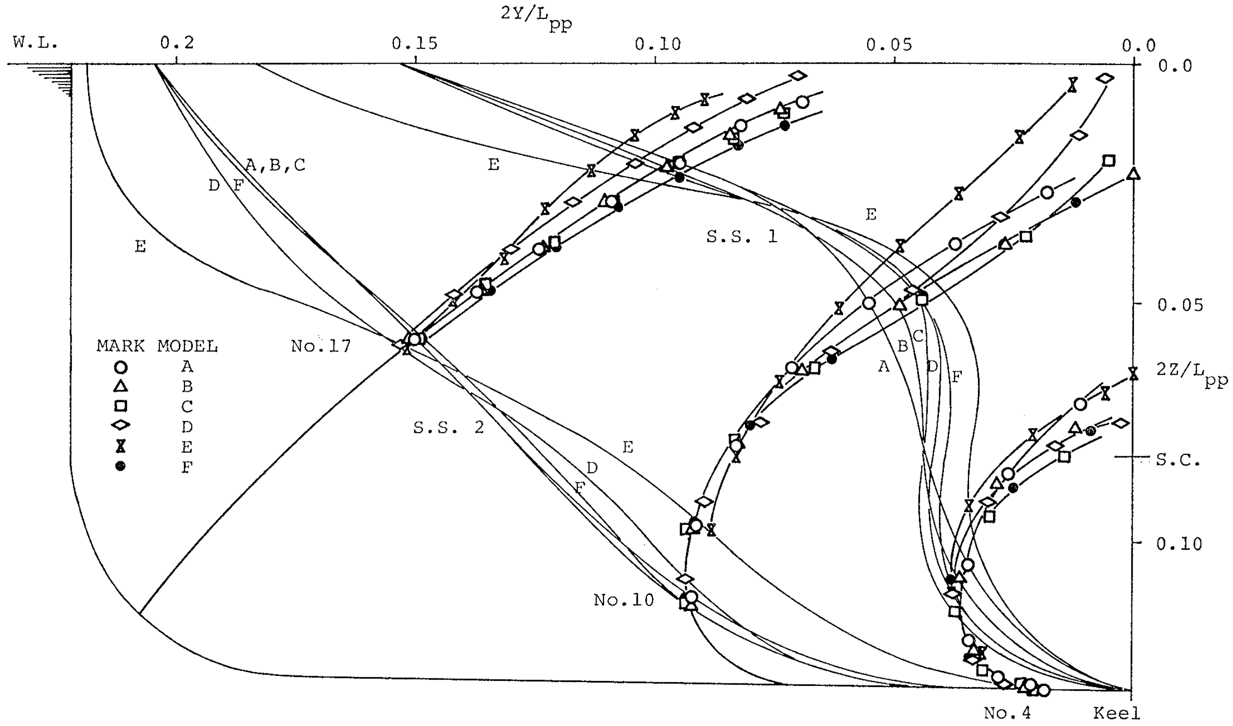

Fig. 5 Comparison of streamline and frameline

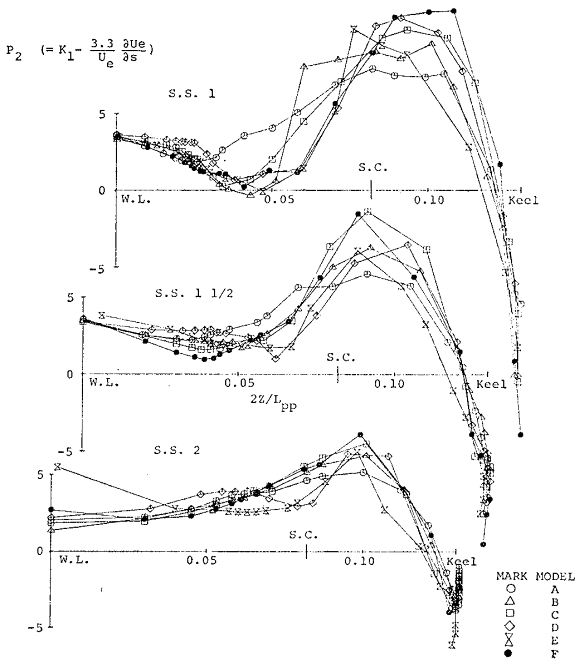

Fig. 6 Modified pressure gradient P_2

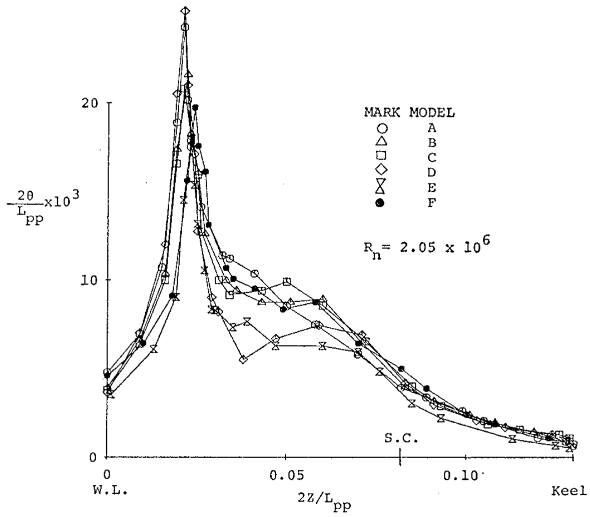

Fig. 7 Momentum thickness at S.S.1

in Table 1. Fig. 5 represents typical frame lines at stern. The other series is 12 tanker forms in SR61, of which the dimensions are listed in Table 2.

Hess and Smith's method is used for the potential flow calculation, and Okuno's method for the boundary layer calculation.

The potential streamlines of SR 183 forms in Fig. 5 indicates the difference of the design

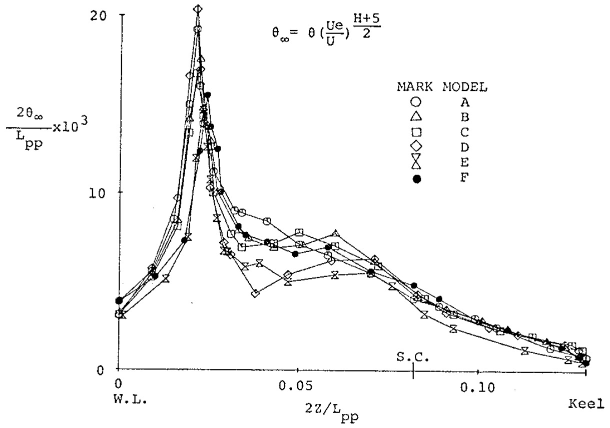

Fig. 8 Distribution of mementum-drag component

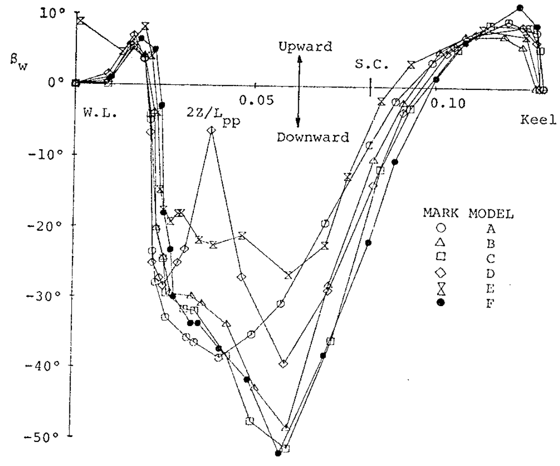

Fig. 10 Wall crossflow at S.S.1

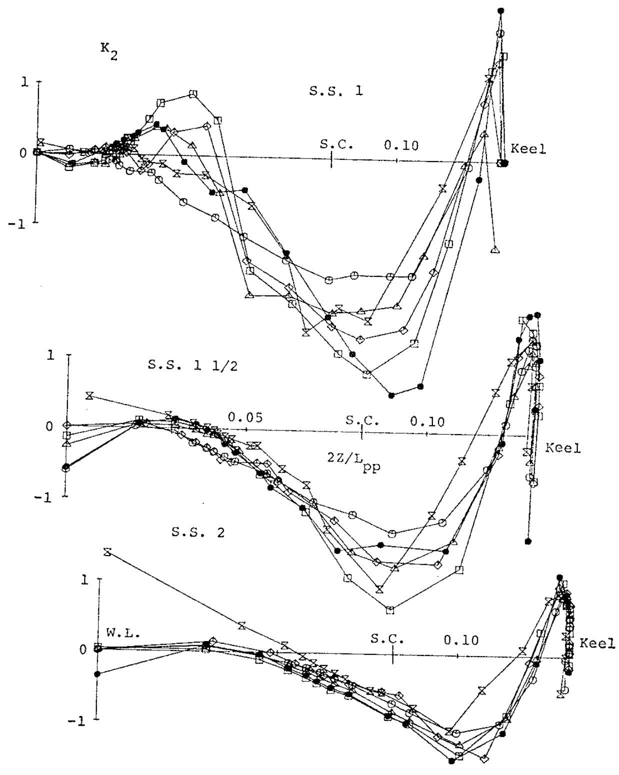

Fig. 9 Streamline curvature K_2

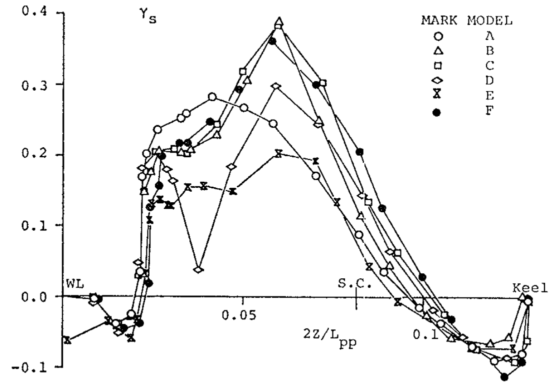

Fig. 11 Circulation density γ_s due to the crossflow in boundary layer at S.S.1

concept for each ship form, i.e., the streamlines of Models B and C go lower near the bulb, and those of Models C, D, and E go upward at the side hull according to the inclination of the frame lines there. The modified pressure gradient P_2 in Fig. 6, the momentum thickness θ in Fig. 7, and in Fig. 8 express corresponding deviations to the difference of hull form. The peak of the momentum thickness appears at the streamline No. 17 which comes from bilge circle, mostly suffers from the effect of the streamline convergence and the pressure gradient.

The streamline curvature in Fig. 9, the wall crossflow angle in Fig. 10, and the circulation density are also related each other. Model E seems to have small crossflow in the whole, since its frame line is highly of buttock-flow type. Fig. 12 shows the profile of the upward inviscid velocity V_n for reference. Figs. 13 and 14 represent longitudinal distributions of the resistance components R_{MOM} and R_{VOR}. To avoid confusion due to the numerical divergence, the value of R_{MOM} is taken at the

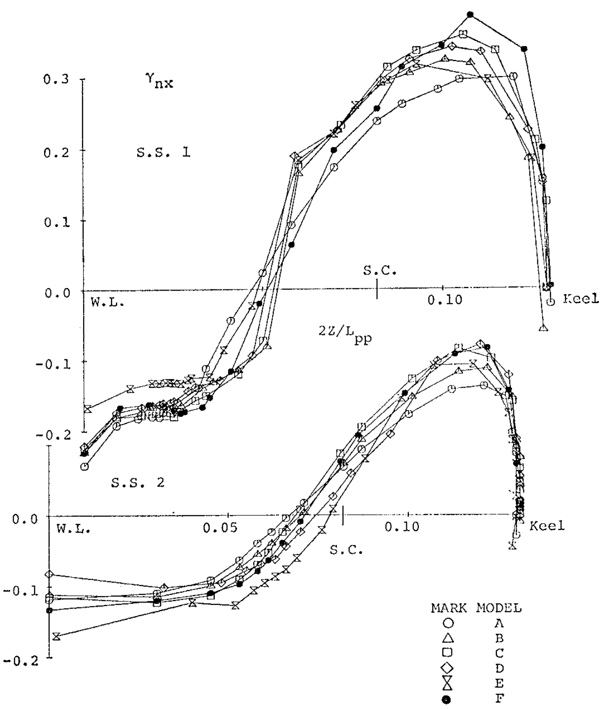

Fig. 12 Circulation density γ_{nx} due to upward inviscid velocity V_n

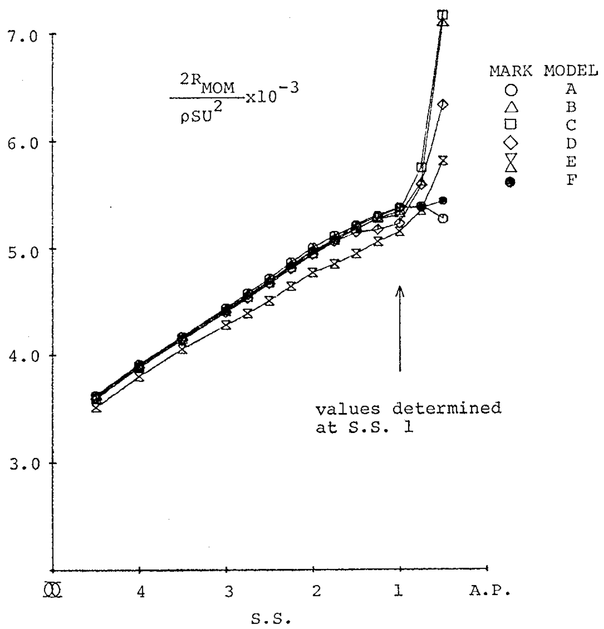

Fig. 13 Momentum resistance R_{MOM}

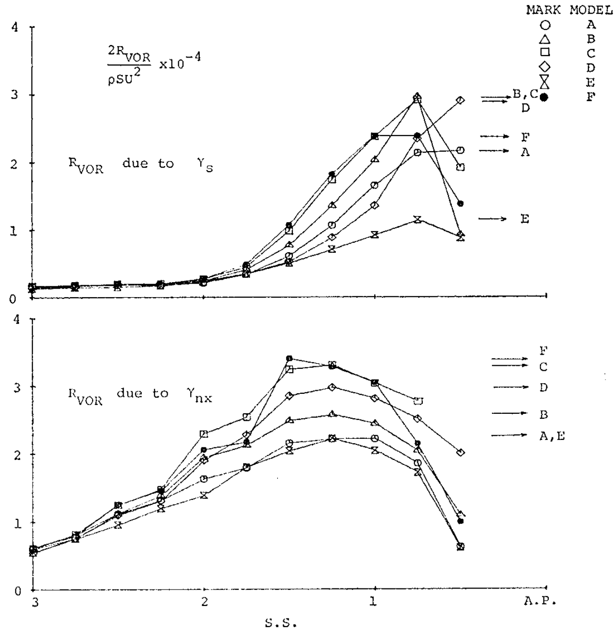

Fig. 14 Vortex resistance R_{VOR}

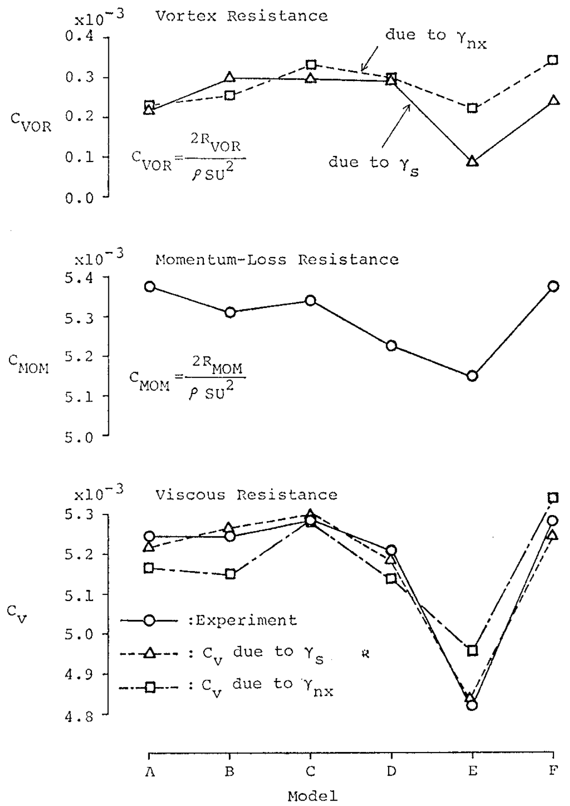

Fig. 15 Comparison of Resistance components

station SS1 in Fig. 13. Taking γ_s, not γ_{nx}, for the circulation density to calculate R_{VOR}, and determining its maximum value as shown in Fig. 14, we have the following regression formula for the series SR183.

$$C_V=0.914C_{MOM}+1.399C_{VOR} \quad (5.1)$$

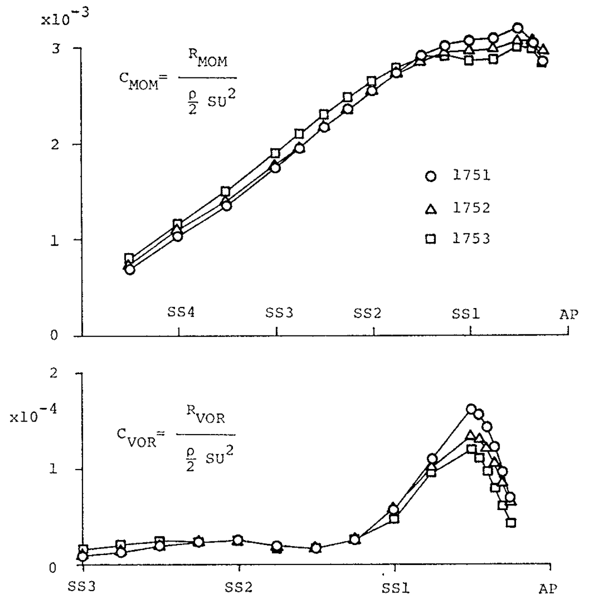

Fig. 16 Distribution of viscous resistance components of SR-61 Series

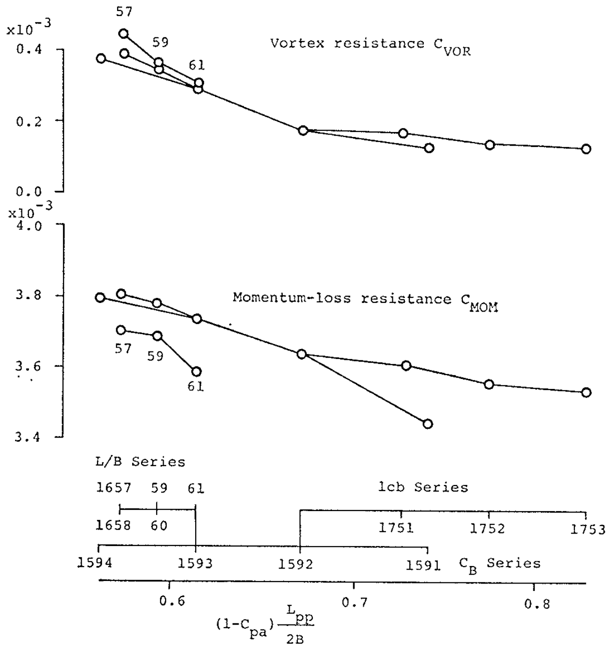

Fig. 17 Viscous resistance components of SR-61 Series

The constants are obtained by fitting the estimated values to the experiment carried out at Sasebo Heavy Industires. The coefficients C_{MOM} and C_{VOR} are in dimensionless form with $1/2\rho SU^2$. Fig. 15 shows a com-

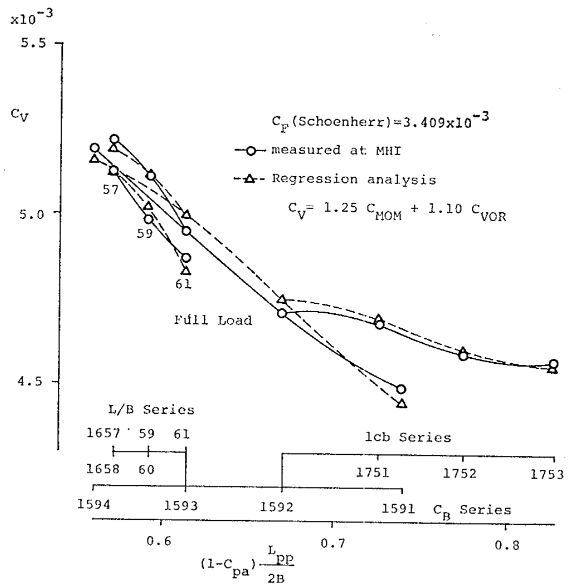

Fig. 18 Viscous resistance of SR-61 Series

parison of the resistance components among the models, in which Model E shows smallest resistance both in the momentum loss and in the vortex resistance. The case in which the value γ_{nx} is taken does not seem so well as case of γ_s.

Figs. 16, 17, and 18 show similar analyses for the series SR61 tanker form. In this case we obtain the regression equation,

$$C_V = 1.25C_{MOM} + 1.10C_{VOR} \tag{5.2}$$

in which the values of the coefficients differ from the former case. For practical use, we have to determine appropriate values for the coefficients according to specified series form.

6. Conclusions

A new approach to predict ship viscous resistance is proposed using existing simple boundary layer calculation method. The following can be concluded.

(i) For axisymmetric swirling wake flow, the second order solutions are obtained. The swirl is associated with a pressure drop and an increment of the wake velocity.

(ii) Taking the pressure drop as the vortex resistance, it damps in the wake, and accordingly the momentum loss increases and approaches to a constant in a far downstream.

(iii) Defining the vortex resistance as its maximum value, it is applied to the ship stern flow. The viscous resistance is assumed to consist of two components, i.e., the momentum loss resistance and the vortex resistance, both of which can be calculated by the boundary layer quantities.

(iv) Importance of the hull distribution of these resistance components is pointed out from the point of hull form improvement. A new parameter, called modified pressure gradient, and the strealine curvature are found to be essential factors for ship boundary layer and viscous resistance developments. And both of these factors are obtainable by inviscid flow calculation.

(v) The present methods are applied to two ship form series, and their applicability is confirmed through comparisons with experiments.

References

1) S. SOEJIMA: Calculation of Thick Boundary Layer Around Ship Stern, Trans., West-Japan Soc. Naval Arch., No. 60, p. 1, Aug. (1980)
2) T. NAGAMATSU: Calculation of Viscous Pressure Resistance of Ships Based on a Higher Order Boundary Layer Theory, Jour., Soc. Naval Arch. Japan, Vol. 147, p. 20, June (1980)
3) K. MURAOKA: Calculation of Viscous Flow around Ship Stern, Trans., West-Japan Soc. Naval Arch., No. 58, p. 235, Aug. (1979)
4) T. HATANO and others: Calculation of Ship Frictional Resistance by Three-Dimensional Boundary Layer Theory, Jour., Soc. Naval Arch. Japan, Vol. 130, pl. 1, Dec. (1971) (in Japanese)
5) Y. HIMENO and I. TANAKA: An Exact Integral Method for Solving Three-Dimensional Turbulent Boundary Layer Equation around Ship Hull, Jour., Kansai Soc. Naval Arch. Japan, No. 159, p. 65, Dec. (1975) (in Japanese)
6) I. TANAKA and Y. HIMENO: First Order Approximation to Three-Dimensional Turbulent Boundary Layer and Its Application to Model Ship Correlation, Jour., Soc. Naval Arch. Japan, Vol. 138, p. 65, Dec. (1975)
7) T. OKUNO: Distribution of Wall Shear Stress and Cross Flow in Three-Dimensional Turbulent Boundary Layer on Ship Hull, Jour., Soc. Naval Arch. Japan, Vol. 139, p. 1, June (1976) (in Japanese)
8) H. SCHLICHTING: Boundary Layer Theory, 7th ed., p. 764, McGraw-Hill (1979)
9) S. HATANO and T. HOTTA: A Second Order Calculation of Three-Dimensional Turbulent Boundary Layer, Trans., West-Japan Soc. Naval Arch., No. 53, p. 33, Mar. (1977) (in Japanese)
10) S. B. S. UBEROI: Viscous Resistance of Ships and Ship Models, Hydro-og Aerodynamisk Laboratorium, Rep. No. Hy-13, S3p. (1969)
11) T. MAGAMATSU: Experimental Study on the Three-Dimensional Turbulent Boundary Layer of a Fine Ship Form Expressed by Means of Conformal Mapping, Trans., West-Japan Soc. Naval Arch., No. 55, p. 27, Mar. (1978)
12) P. S. GRANVILLE: The Calculation of Viscous Drag of Bodies of Revolution, David Taylor Model Basin Report, No. 849 (1953)
13) J. L. HESS: On the Problem of Shaping an Axisymmetric Body to Obtain Low Drag at Large Reynolds Numbers, Jour. Ship Res., Vol. 20, No. 1, Mar. (1976)
14) G. H. HOFFMAN: A Modified Displacement-Body Method for Treating the Axisymmetric Strong-Interaction Problem, Jour. Ship Res., Vol. 24, No. 2 (1980)
15) H. SASAJIMA and others: On Stern Flow Field of Full Ship Forms and Induced Drag due to Bilge Vortices, Jour. Soc. Naval Arch. Japan, Vol. 128, p. 43, Dec. (1970) (in Japanese)
16) J. C. TATINCLAUX: Experimental Investigation of the Drag Induced by Bilge Vortices, Schiffs Technik, Band 17, Heft 87 (1970)
17) H. TANAKA: Resistance of the Submerged Bodies Running Near a Free Surface, Jour. Soc. Naval Arch. Japan, Vol. 136, p. 1, Dec. (1974) (in (Japanese)
18) M. BESSHO: Study into Frame Line Configuration, Jour. Soc. Naval Arch. Japan, Vol. 122, p. 43 (1967) (in Japanese)
19) M. BESSHO and T. MIZUNO: A Study of Full Ship Forms, Jour., Kansai Soc. Naval Arch., Japan, No. 117, p. 23, June (1965) (in Japanese)
20) M. BESSHO and T. MIZUNO: ditto (The Second Report), Jour., Kansai Soc. Naval Arch., Japan, No. 121, p. 15, June (1966) (in Japanese)
21) Japan Shipbuilding Research Association, SR 183 Com. Report, No. 342 (1981) and No. 348 (1982) (in Japanese)
22) Japan Shipbuilding Research Association, SR61 Com. Report, No. 67 (1969) (in Japanese)
23) L. ROSENHEAD: Laminar Boundary Layers, p.

455, Oxford Univ. Press (1963)
24) Y. HIMENO: Displacement Effect of Three-Dimensional Turbulent Boundary Layer and Wake of Ship, Proc., International Seminar on Wave Resistance, Kansai, Dec. (1976)